Development 134, 3461-3471 (2007) doi:10.1242/dev.004556

Inactivation of serine protease Matriptase1a by its inhibitor Hai1 is required for epithelial integrity of the zebrafish epidermis

Thomas J. Carney[1], Sophia von der Hardt[1], Carmen Sonntag[1], Adam Amsterdam[2], Jacek Topczewski[3], Nancy Hopkins[2] and Matthias Hammerschmidt[1,4,*]

Epithelial integrity requires the adhesion of cells to each other as well as to an underlying basement membrane. The modulation of adherence properties is crucial to morphogenesis and wound healing, and deregulated adhesion has been implicated in skin diseases and cancer metastasis. Here, we describe zebrafish that are mutant in the serine protease inhibitor Hai1a (Spint1la), which display disrupted epidermal integrity. These defects are further enhanced upon combined loss of *hai1a* and its paralog *hai1b*. By applying in vivo imaging, we demonstrate that Hai1-deficient keratinocytes acquire mesenchymal-like characteristics, lose contact with each other, and become mobile and more susceptible to apoptosis. In addition, inflammation of the mutant skin is evident, although not causative of the epidermal defects. Only later, the epidermis exhibits enhanced cell proliferation. The defects of *hai1* mutants can be phenocopied by overexpression and can be fully rescued by simultaneous inactivation of the serine protease Matriptase1a (St14a), indicating that Hai1 promotes epithelial integrity by inhibiting Matriptase1a. By contrast, Hepatocyte growth factor (Hgf), a well-known promoter of epithelial-mesenchymal transitions and a prime target of Matriptase1 activity, plays no major role. Our work provides direct genetic evidence for antagonistic in vivo roles of Hai1 and Matriptase1a to regulate skin homeostasis and remodeling.

KEY WORDS: Hai1, Spint1, Matriptase1, St14, HGF, Met, Epidermis, Scattering, EMT, Zebrafish

INTRODUCTION

Serine proteases regulate diverse cellular behaviors in numerous contexts, including in development, tumorigenesis and wound healing (reviewed in Kataoka et al., 2002). This is achieved either by cleaving a pro-protein to a functional form or by the inactivation/degradation of a substrate. Strict control of protease activity and expression is thus crucial for proper tissue ontogeny and homeostasis, and deregulated activity of a number of proteases is associated with human disease states.

Matriptase1 [also known as Matriptase, membrane-type serine protease 1 (MT-SP1) and Suppression of tumorigenicity 14 (St14)] is a type II transmembrane serine protease, first identified in human breast cancer cells (Lin et al., 1999b; Shi et al., 1993), and is expressed in a broad range of epithelia (Kim et al., 1999; Oberst et al., 2001; Oberst et al., 2003; Takeuchi et al., 1999). Increasing interest in this enzyme has centered on its strong correlation with epithelial tumor progression and the deleterious effects resulting from altering its activity levels in vivo (reviewed in List et al., 2006). One crucial regulator of the proteolytic activity of Matriptase1 has been shown, in vitro, to be the membrane-associated serine protease inhibitor Hepatocyte growth factor activator inhibitor 1 (Hai1, also known as Spint1) (Benaud et al., 2001; Lin et al., 1999a), which is almost invariably co-expressed with Matriptase1 (Oberst et al., 2001) and was first described as an inhibitor of the circulating serine protease Hepatocyte growth factor activator (Hgfa, also known as Hgfac) (Shimomura et al., 1997). The inhibitory activity of Hai1 is conferred via its extracellular Kunitz domains, which bind directly to the protease sites (Denda et al., 2002; Kirchhofer et al., 2003). Via the inhibition of both Matriptase1 and Hgfa, Hai1 is thought to be able to attenuate cell motility via limiting serine protease-mediated activation of the potent motogen Hepatocyte growth factor (Hgf, also known as Scatter factor, Sf) (Parr and Jiang, 2006). In addition to Hgf, Matriptase1 has been shown to activate other proteins and zymogens, such as urokinase plasminogen activator (uPA, also known as Plau), protease activated receptor 2 (PAR2, also known as F2rl1), matrix metalloprotease 3 (MMP3), insulin-like growth factor binding protein-related protein-1 (IGFBP-rP1, also known as IGFBP7) and CUB domain containing protein 1 (CDCP1) (Ahmed et al., 2006; Bhatt et al., 2005; Jin et al., 2006; Lee et al., 2000; Takeuchi et al., 2000). Furthermore, Matriptase1 can degrade extracellular matrix and structural proteins, including Laminin and Fibronectin (Satomi et al., 2001). In vitro models have shown that Matriptase1 induces cell scattering and invasion via both Hgf-Met-dependent and -independent mechanisms (Forbs et al., 2005); however, the in vivo relevance of these downstream pathways remains largely untested.

Knockout of *matriptase1* in the mouse produced epidermal structural and barrier defects due to insufficient processing of profilaggrin (Flg) to a mature form in cornifying outer keratinocytes (List et al., 2002; List et al., 2003). The *hai1*-knockout mouse dies in utero because of placental defects underscored by a loss of epithelial integrity of chorionic trophoblasts (Tanaka et al., 2005) and the underlying basement membrane (Fan et al., 2007). These placental defects are due to deregulated matriptase1 activity, as confirmed by a double-knockout strategy (Szabo et al., 2007). Similarly, squamous cell carcinogenesis caused by overexpressing

[1]Max-Planck-Institute of Immunobiology, Stuebeweg 51, D-79108 Freiburg, Germany. [2]Center of Cancer Research, Massachusetts Institute of Technology, Cambridge, MA 02139, USA. [3]Children's Memorial Research Center, Northwestern University, Feinberg School of Medicine, Chicago, IL 60614, USA. [4]Institute for Developmental Biology, University of Cologne, D-50923 Cologne, Germany.

*Author for correspondence (e-mail: hammerschmid@immunbio.mpg.de)

Accepted 26 June 2007

matriptase1 in the mouse skin was rescued by the concomitant overexpression of Hai1 (List et al., 2005). However, it remains to be demonstrated whether Hai1 repression of Matriptase1 is necessary for normal epidermal development.

Here, we describe the roles of two Hai1 and a Matriptase1 homologues during skin development in the zebrafish (*Danio rerio*), based on mutant and antisense-mediated loss-of-function studies. During embryonic and larval stages, the zebrafish epidermis is bi-layered, consisting of a basal and an outer layer of keratinocytes (Le Guellec et al., 2004). As in mammals, basal keratinocytes are attached to the basement membrane via hemi-desmosomes and to each other via desmosomes (Sonawane et al., 2005), and are characterized by the expression of the p53-related transcription factor ΔNp63 (also known as Tp73l – Zebrafish Information Network) (Bakkers et al., 2002). Zebrafish *hai1a* (also known as *spint1la* – Zebrafish Information Network; GenBank accession number NM_213152), *hai1b* (*spint1lb*; GenBank accession number EF424430) and *matriptase1a* are expressed in the developing basal layer of the epidermis. Via live imaging and marker analysis, we describe both epithelial and inflammatory skin phenotypes caused by loss of Hai1 activity, and thus provide direct genetic evidence for an essential role of Hai1 to maintain epithelial integrity of the epidermis during development. Furthermore, by inactivating both Hai1 and Matriptase1a, we demonstrate that Hai1 fulfills its epidermal function by blocking Matriptase1a. Finally, we show that deregulated Matriptase1a activity does not require the Hgf receptor Met or related receptors to induce the observed scattering of *hai1* mutant keratinocytes, indicating that other Matriptase1 target proteins must be involved.

MATERIALS AND METHODS

Fish husbandry

The *hai1a* allele *hi2217* was isolated during an insertional mutagenesis screen (Amsterdam et al., 1999). *hai1a* mutant embryos were obtained from heterozygous or homozygous parents. Embryos lacking early Smad5 function and specification of ectodermal precursor cells were obtained by crossing mothers heterozygous for the dominant-negative allele *dtc24* with wild-type males (Hild et al., 1999). The *Tg(bactin:hras-egfp)* (allele *vu119*) and the *Tg(fli1a:egfp)* (allele *y1*) transgenic lines have been described previously (Cooper et al., 2005; Lawson and Weinstein, 2002).

Cell transplantations

Clusters of mGFP-labeled basal keratinocytes were obtained by homotypic (wild type→wild type; *hai1a* morphant→*hai1a* morphant; *hai1a+hai1b* morphant→*hai1a+hai1b* morphant) transplantation of non-neural ectodermal cells from *Tg(bactin:hras-egfp)* transgenic donor embryos into non-transgenic hosts. Recipients were developed to 24 hours post fertilization (hpf), mounted in 1.5% low melting point agarose under E3 medium and analyzed by time-lapse confocal microscopy.

RNA isolation, cDNA synthesis, RT-PCR and 5′RACE

Total RNA was isolated from embryos using Trizol-LS (Invitrogen, CA) and cDNA synthesized with SuperscriptII reverse transcriptase (Invitrogen). Sequences corresponding to zebrafish orthologs of *hai1a*, *hai1b*, *prgfr3* and *hgfa* were obtained from the zebrafish genome (Ensembl, Sanger Center), and were amplified via reverse transcriptase (RT)-PCR. To determine the full 5′ sequence of *hai1b* and *prgfr3* cDNAs, 5′RACE was performed using the SMART RACE kit (BD Biosciences, CA).

Cloning of cDNAs, probe synthesis and heat-shock treatment

Zebrafish cDNA fragments for *hai1a*, *hai1b* and *prgfr3* obtained by RT-PCR were cloned into pCRII-TOPO (Invitrogen) or pGEM-T Easy (Promega, WI). cDNA clones of *matriptase1a* (IMAGp998P136587), *matriptase1b* (IMAGp998H0614296) and *ron* (IMAGp998M1514792) were obtained from RZPD (Berlin, Germany). The *matriptase1a* insert was shuttled into pCRII-TOPO. For probe synthesis, plasmids were linearized with *Nco*I (*hai1b, hgfa*), *Not*I (*matriptase1a*, *hai1a*, *prgfr3*), *Eco*RI (*matriptase1b*) or *Sma*I (*ron*). Probes for *hai1a*, *hai1b*, *matriptase1a*, *prgfr3* and *hgfa* were synthesized using Sp6 RNA polymerase (Roche, Mannheim, Germany), and probes for *matriptase1b* and *ron* with T7 RNA polymerase.

For *matriptase1a* overexpression studies, the heat-inducible construct *pTol2-hse-GFP/matriptase1a* was generated, cloning the *matriptase1a* cDNA into the bicistronic vector pSGH2 (Bajoghli et al., 2004), which, in addition to *matriptase1a*, drives expression of GFP under the control of heat-shock elements (hse). Subsequently, the cassette was ligated into vector pT2AL200R150G, which contains Tol2 recognition sites to allow early genomic integration and widespread expression upon co-injection with Tol2 transposase mRNA (Kawakami et al., 2004; Urasaki et al., 2006). For transgene activation, injected embryos were transferred from 28°C to 39°C from 20-22 hpf.

In situ hybridization and immunostainings

In situ hybridizations were performed as previously described (Hammerschmidt et al., 1996), using probes for *hai1a*, *hai1b*, *matriptase1a*, *myoD* (Weinberg et al., 1996), *met* (Haines et al., 2004), *pu.1* (*spi1*) (Lieschke et al., 2002), *lcp1* (Herbomel et al., 1999), *mpx* (Lieschke et al., 2001) and *e-cadherin* (*cdh1*) (Babb et al., 2001). Whole-mount antibody stainings were visualized with the Vectastain ABC kit (Axxora) as described (Hammerschmidt et al., 1996), or with fluorescent secondary antibodies. For combined colorimetric in situ hybridizations and immunostainings (Fig. 1F,G,I and Fig. 7A), embryos underwent standard in situ hybridization, followed by a fixation for 4-6 hours in 4% paraformaldehyde/PBS, and a standard immunostaining (Hammerschmidt et al., 1996). Antibodies, dilutions used and sources were as follows: 4A4 anti-p63 (1:200, Santa Cruz), anti-GFP (1:400, Invitrogen), anti-E-cadherin (1:200, BD Biosciences), Alexa-Fluor-546 goat anti-mouse (1:400, Invitrogen) and Alexa-Fluor-488 goat anti-rabbit (1:400, Invitrogen).

Western blotting

Protein extracts of embryos were separated by 8% SDS-PAGE under reducing conditions and transferred to nitrocellulose membrane. Anti-E-cadherin antibody was used at 1:5000 dilution, and secondary HRP-coupled goat anti-mouse antibody (Dianova, Hamburg, Germany) at 1:10000.

Morpholino oligonucleotides (MOs)

MOs were obtained from Gene Tools (Philomath, OR) and diluted in Danieau's buffer (Nasevicius and Ekker, 2000). MO solution (1.5 nl) was injected per embryo. *hai1a* MO (5′-ACCCTGAGTAGAGCCAGAGT-CATCC-3′) and *matriptase1a* MO (5′-AACGCATTCCTCCATCCATA-GGGTC-3′) were injected at 100 μM; *ron* MO (5′-AACAAGGTCTTTGG-GCTGATGAACA-3′) and *prgfr3* MO (5′-CTAAATGAGTGGCCCA-ATGGACCAT-3′) at 200 μM; and *hai1b* MO (sequence 5′-CACC-ACGAACCCATTTTTGATTGAT-3′), the *met* MO (Haines et al., 2004) and *pu.1* MO (Rhodes et al., 2005) at 500 μM.

BrdU and acridine orange stainings

Epidermal cell proliferation was assessed by BrdU incorporation followed by combined α-p63 and α-BrdU antibody detection as described (Lee and Kimelman, 2002). Apoptotic cells were visualized by acridine orange staining as described (Furutani-Seiki et al., 1996).

Microscopy

Fluorescent images were taken with a Zeiss Confocal microscope (LSM510 META); all other microscopy was performed on a Zeiss Axiophot.

RESULTS

An insertion in the zebrafish *hai1a* locus disrupts *hai1a* gene activation and causes specific epidermal defects

To identify genes with essential functions during zebrafish skin development, we performed an antibody-based screen on a previously described bank of insertional mutants (Amsterdam et al., 1999), staining larvae at 48 hours post fertilization (hpf) for p63 protein, a marker of basal keratinocytes (Lee and Kimelman, 2002).

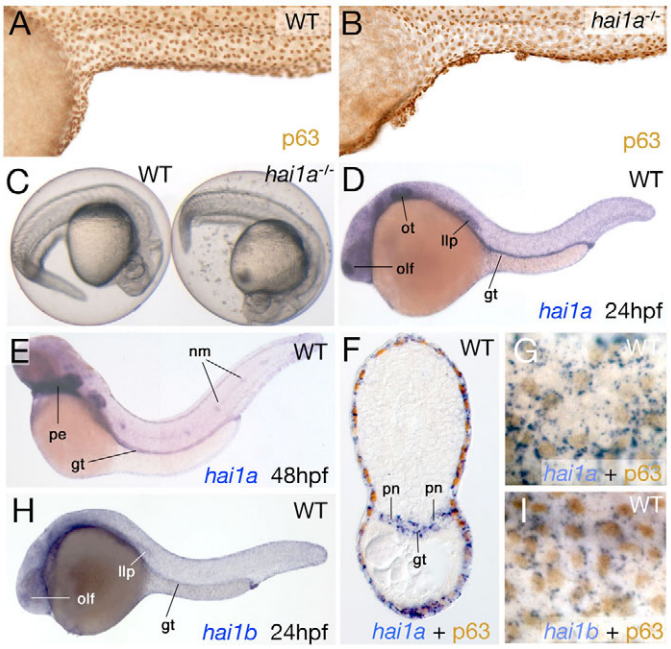

Fig. 1. *hai1a* is expressed in basal keratinocytes and is required for the proper development of the epidermis. (**A**,**B**) Lateral views of the trunk of a wild-type sibling (WT; A) and a homozygous *hi2217* embryo (*hai1a*$^{-/-}$; B) at 48 hpf, after anti-p63 immunolabeling of basal keratinocytes. (**C**) Shedding of cells into the chorion is evident in *hi2217* homozygotes (right embryo), compared with no shedding in the wild-type sibling (left embryo) from 24 hpf. (**D**,**E**,**H**) In situ hybridization showing the expression of *hai1a* at 24 hpf (D) and 48 hpf (E), and of *hai1b* at 24 hpf (H). The *hai1a* and *hai1b* expression domains in olfactory epithelium (olf), otic epithelium (ot), gut (gt), lateral line primordium (llp), neuromasts (nm) and pharyngeal endoderm (pe) are indicated. (**F**,**G**,**I**) Cross-section through the posterior trunk of a 24 hpf wild-type embryo after double staining for *hai1a* mRNA (blue) and p63 protein (brown) (F), and magnified views of the trunk epidermis of a 24 hpf wild-type embryo after double staining for *hai1a* (G) or *hai1b* (I) (blue) and p63 protein (brown). In F, the *hai1a* expression domains in the pronephric ducts (pn) and gut (gt) are indicated.

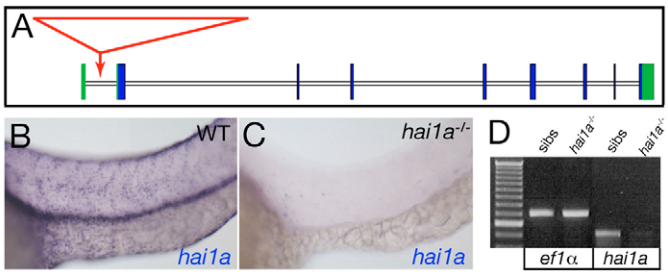

Fig. 2. The insertion in *hi2217* abrogates *hai1a* transcription. (**A**) Structure of the *hai1a* gene showing the viral insertion site in the *hi2217* allele (red). Exons are boxed with coding and non-coding sequences in blue and green, respectively. The viral insertion (red arrow) occurs in the first intron upstream of the first coding exon. (**B**,**C**) Lateral views of the trunk epidermis of a wild-type sibling (WT; B) and a *hi2217* homozygote (C) at 24 hpf, after *hai1a* in situ hybridization. (**D**) Reverse transcriptase (RT)-PCR analysis of *hi2217* homozygotes (lanes 3,5) and wild-type siblings (lanes 2,4) at 24 hpf, demonstrating a strong reduction in *hai1a* transcript levels in mutants compared with siblings, whereas *ef1a* levels are identical. Lane 1, 100 bp ladder.

One mutant that we identified, *hi2217*, displayed aggregations of p63-positive keratinocytes (Fig. 1B) compared with the even distribution of these cells in wild-type siblings (Fig. 1A). Such aggregates were most prominent on the yolk sac and yolk extension, and were already visible at 24 hpf (see below). In addition, skin cells were seen floating in the chorion of mutant embryos from 24 hpf (Fig. 1C).

By determining the flanking sequences of the viral DNA in *hi2217* mutants (Amsterdam et al., 2004), we found that the mutagenic insertion had occurred in intron 1 of the *hai1a* gene, which is homologous to the hepatocyte growth factor activator inhibitor 1 (*Hai1*, *Spint1*) gene in mammals. Because the insertion is upstream of the first coding exon (Fig. 2A), it most probably leaves the structure and function of the Hai1a protein intact. However, it attenuated *hai1a* transcription to below detection thresholds. At 24 hpf and 48 hpf, wild-type embryos displayed strong *hai1a* expression in epithelia such as the epidermis, the olfactory epithelium, the otic vesicle, the gut, and the lateral line primordium and neuromasts (Fig. 1D,E). Combination with anti-p63 immunostaining revealed that, within the epidermis, *hai1a* transcripts were present around the p63-positive nuclei, pointing to expression in the basal layer (Fig. 1F,G). However, in contrast to wild-type siblings (Fig. 2B), no *hai1a* expression could be detected by in situ hybridization in *hai1a* mutants between 24 and 72 hpf (Fig. 2C; and data not shown). Consistent results were obtained using semi-quantitative reverse transcriptase (RT)-PCR of extracts from whole-mutant and wild-type sibling embryos at 24 hpf (Fig. 2D), indicating that the viral insertion strongly abrogates *hai1a* transcription or transcript stability. As further evidence that the viral insertion was causative of the observed skin phenotype, we injected an antisense morpholino oligonucleotide (MO) targeting the *hai1a* translation start site (*hai1a* MO) into wild-type embryos, which led to a robust phenocopy of the epidermal defects (compare Fig. 3G-I with 3A-F).

In addition to the epidermis, *hai1a* mutants also displayed disrupted morphology of the olfactory epithelium (see Fig. S1A-C in the supplementary material), another ectodermal derivative displaying prominent *hai1a* expression (Fig. 1D), whereas, in the pronephric ducts and the gut, *hai1a*-positive epithelia (Fig. 1D,F) derived from the mesoderm or endoderm, respectively, appeared unaffected by the mutation (see Fig. S1D-G in the supplementary material).

hai1a acts in partial redundancy with its paralog, *hai1b*

By searching genomic and EST databases of the zebrafish, we identified a second zebrafish *hai1* gene, named *hai1b*. On the amino acid level, Hai1a and Hai1b are 43% identical, and both are more similar to mouse Hai1 (34 and 37% identity, respectively) than to mouse Hai2 (also known as Spint2 – Mouse Genome Informatics; both 14% identity), indicating that they are true paralogs that might have arisen from the genome duplication that has occurred during teleost evolution (Postlethwait et al., 1998).

Whole-mount in situ hybridizations revealed that, as is *hai1a* (Fig. 1D,G), *hai1b* is expressed in the basal epidermis (Fig. 1H,I), raising the possibility that Hai1a and Hai1b might have partly redundant functions. Therefore, we inactivated *hai1b* by injecting a specific *hai1b* MO into wild-type or *hai1a* mutant or morphant embryos. *hai1b* morphant embryos displayed completely normal morphology and normal p63 expression (Fig. 3J-L), whereas the skin defects of *hai1a, hai1b* double-morphant embryos (Fig. 3M-O) were much

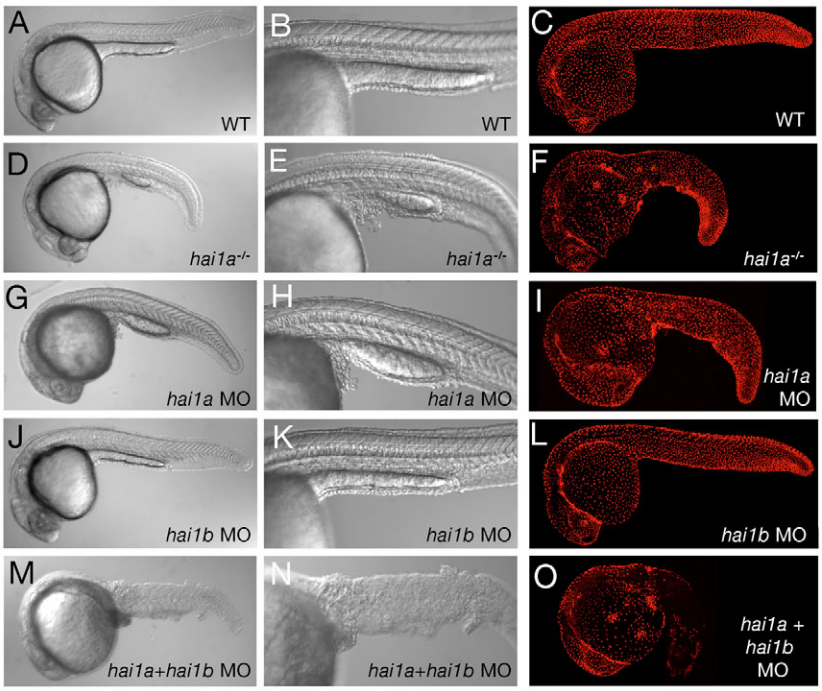

Fig. 3. Keratinocyte aggregation and shedding caused by the loss of Hai1a is further enhanced by the concomitant loss of its paralog, Hai1b. All panels show embryos at 24 hpf; wild-type siblings (WT; **A-C**), *hai1a* mutants (**D-F**), *hai1a* morphants (**G-I**), *hai1b* morphants (**J-L**) and *hai1a* mutants injected with *hai1b* MOs (**M-O**). Shown are lateral views of live embryos using Nomarski optics at low power (A,D,G,J,M) to assess overall embryo morphology, and at higher magnification (B,E,H,K,N) to assess epidermal defects in the trunk/tail regions, and lateral views of embryos after immunofluorescent detection of the basal epidermal marker protein p63 (C,F,I,L,O; merged stacks of confocal images).

more severe than in *hai1a* single mutants (Fig. 3D-F) or morphants (Fig. 3G-I). In 24 hpf *hai1a* single mutants, aggregates of basal keratinocytes were largely restricted to the yolk sac, the yolk extension and the ventral trunk, whereas cell shedding mainly occurred at the border between the yolk sac and yolk extension (Fig. 3D,E). By contrast, *hai1a, hai1b* double-morphant embryos displayed keratinocyte aggregations and cell shedding in all regions of the skin (Fig. 3M-O). At 24 hpf, many embryos had already lysed (Table 1) or were about to die, most probably due to the loss of functional skin, whereas *hai1a* mutants often recovered quite well, with skin aggregations and lesions only remaining in the forming body fins (data not shown). Together, these data indicate that Hai1b, although dispensable during normal skin development, can, to some extent, compensate for the loss of Hai1a.

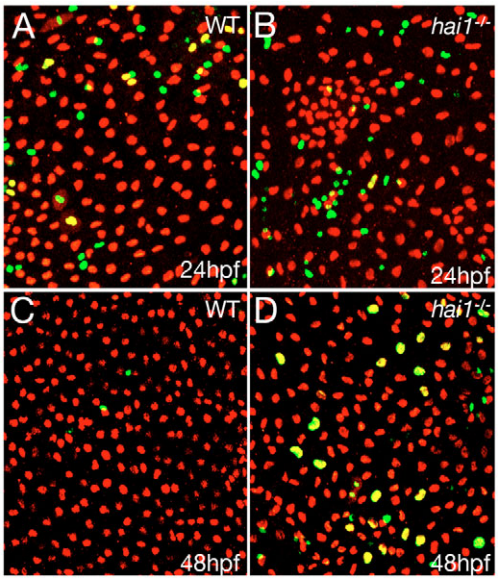

Fig. 4. Enhanced basal keratinocyte proliferation in *hai1a* mutant embryos occurs subsequent to epidermal cell aggregation. (**A-D**) Confocal images of ventral yolk epidermis of wild-type siblings (WT; A,C) and *hai1a* mutants (B,D) at 24 hpf (A,B) and 48 hpf (C,D), after BrdU labeling of proliferating cells (green) and anti-p63 immunolabeling of basal keratinocytes (red).

Epidermal aggregates form because of a loss of epidermal and an acquisition of mesenchymal-like properties, whereas epidermal hyper-proliferation occurs only secondarily

To study whether the formation of keratinocyte aggregates in *hai1a* mutants might be caused by an over-proliferation of basal cells, we carried out BrdU pulse labeling at different time points of development, combined with anti-p63 immunostainings to specifically mark basal keratinocytes. BrdU labeling for 4 hours from 20 hpf and staining at 24 hpf revealed a moderate number of proliferating cells among the evenly spaced basal keratinocytes of wild-type siblings (Fig. 4A). In *hai1a* mutants, the number of BrdU and p63 double-positive cells was not noticeably increased (Fig. 4B). Importantly, nascent aggregates of basal keratinocytes consisted solely of BrdU-negative cells (Fig. 4B). However, at 48 hpf, similar 4 hour BrdU pulse experiments revealed a significant increase in the number of proliferating basal keratinocytes in *hai1a* mutants (Fig. 4D), whereas epidermal proliferation had largely ceased in wild-type siblings (Fig. 4C). In conclusion, *hai1a* mutant basal keratinocytes display hyper-proliferation, which, however, occurs too late to account for the initial aggregate formation.

Another explanation for aggregate formation could be a redistribution of basal cells. In line with this notion, p63-positive cells adjacent to the aggregates appeared sparser than in unaffected skin (compare Fig. 4B with 4A). Such redistribution would require that cells give up their initial epithelial organization and acquire mesenchymal-like properties. To examine this possibility, we carried out time-lapse confocal microscopy of clusters of fluorescently labeled basal keratinocytes in wild-type and *hai1a* mutant or

Table 1. The phenotypes of *hai1a* mutants, *hai1a* morphants, and embryos lacking both Hai1a and Hai1b activity are rescued upon (co-)injection of *matriptase1a* MO

		Phenotype (*n*)						
hai1a genotype of parents	MO injection	WT	*hai1* normal	*hai1* strong	Lysed	*n* (total)	% WT	# exps
+/–	–	63	20	0	0	83	75.9	2
+/–	*matriptase1a*	252	3	0	0	255	98.8	2
–/–	–	0	72	0	0	72	0	2
–/–	*matriptase1a*	153	0	0	0	153	100	2
+/+	*hai1a*	8	66	0	0	74	10.8	1
+/+	*hai1a* + *matriptase1a*	167	6	0	0	173	96.5	1
–/–	*hai1b*	0	0	63	41	104	0	2
–/–	*hai1b* + *matriptase1a*	56	48	45	22	171	32.7	2

Compare results of table with those shown in Fig. 7. Phenotypes were evaluated at 24 hpf, based on skin morphology. *n*, number of embryos; % WT, percentage of embryos with wild-type phenotype; # exps, number of evaluated experiments.

morphant embryos from 24 hpf. Regardless of the recorded region, wild-type cells showed typical epithelial characteristics. They were of regular polygonal shapes and remained tightly associated with their neighbors and in fixed locations relative to each other during the entire recorded time (90 minutes; Fig. 5A; in 4/4 movies of transplanted cells). Depending on the region within the embryo, cells from *hai1a* morphant basal keratinocytes displayed a strikingly different behavior. On the yolk sac (data not shown) and in the ventral trunk dorsal to the yolk sac extension, they had less regular and more fibroblastoid cell shapes, changed positions relative to each other, broke contacts to adjacent cells, and formed highly dynamic lamellipodia-like cell protrusions, as normally seen in mesenchymal cells (Fig. 5B; in 5/5 movies; see Fig. 6G for an indication of recorded region). However, this behavior was only observed in regions that are highly susceptible to aggregate formation, whereas regions of *hai1a* morphants that appeared

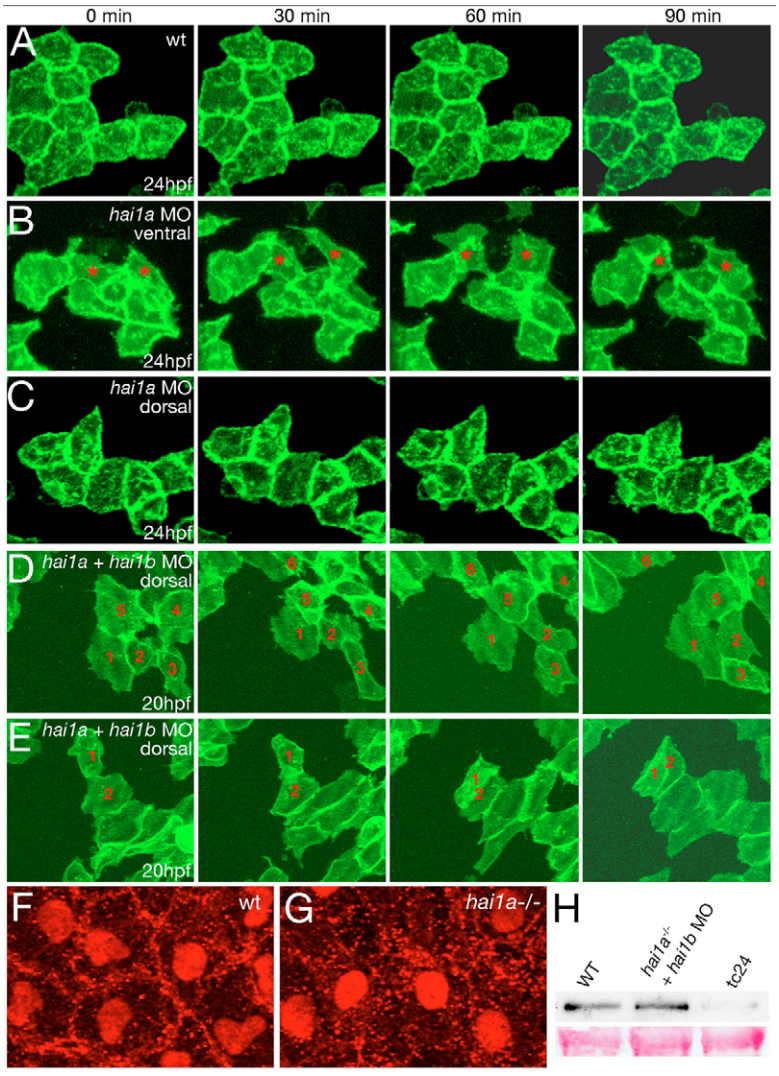

Fig. 5. Loss of Hai1 activity abrogates the epithelial properties of basal keratinocytes. (**A-E**) Stills of in vivo time-lapse recordings of clusters of basal keratinocytes labeled with membrane-bound GFP, at the indicated times after 24 hpf (A-C) or 20 hpf (D,E); wild-type sibling (wt; A; see Movie 1 in the supplementary material); *hai1a* morphants (B,C; see Movies 2 and 3 in the supplementary material); and *hai1a* + *hai1b* double morphants (D,E; see Movies 4 and 5 in the supplementary material). Epidermal cells in the ventral regions of a *hai1a* morphant (B) display a mesenchymal-like behavior (examples indicated by asterisks; recorded region indicated in Fig. 6G). By contrast, epidermal cells in more-dorsal/posterior regions (C) form a rigid epithelium, as in wild-type embryos (A). In embryos lacking both Hai1a and Hai1b, motility and fibroblastoid behavior of basal keratinocytes is further enhanced, evident much earlier and now also seen in dorsal trunk/tail regions (D; individual keratinocytes labeled with numbers). Often, cells migrate on top of each other (E; cells 1 and 2). (**F**,**G**) Ventral confocal views of yolk epidermis of a 24 hpf wild-type sibling (F) and a *hai1a* mutant embryo (G), with immunofluorescent detection of E-cadherin (E-cad) and p63, marking nuclei of basal keratinocytes. (**H**) Anti-E-cad western blots of embryonic extracts from 24 hpf wild-type siblings (left lane) and *hai1a* mutants injected with *hai1b* MO (middle lane), revealing unaltered E-cad protein levels in double-deficient embryos. By contrast, offspring of *smad5*^{dtc24} heterozygous mothers (Hild et al., 1999), which, according to anti-p63 immunostainings, lack basal keratinocytes (data not shown), display strongly reduced E-cad protein levels (right lane).

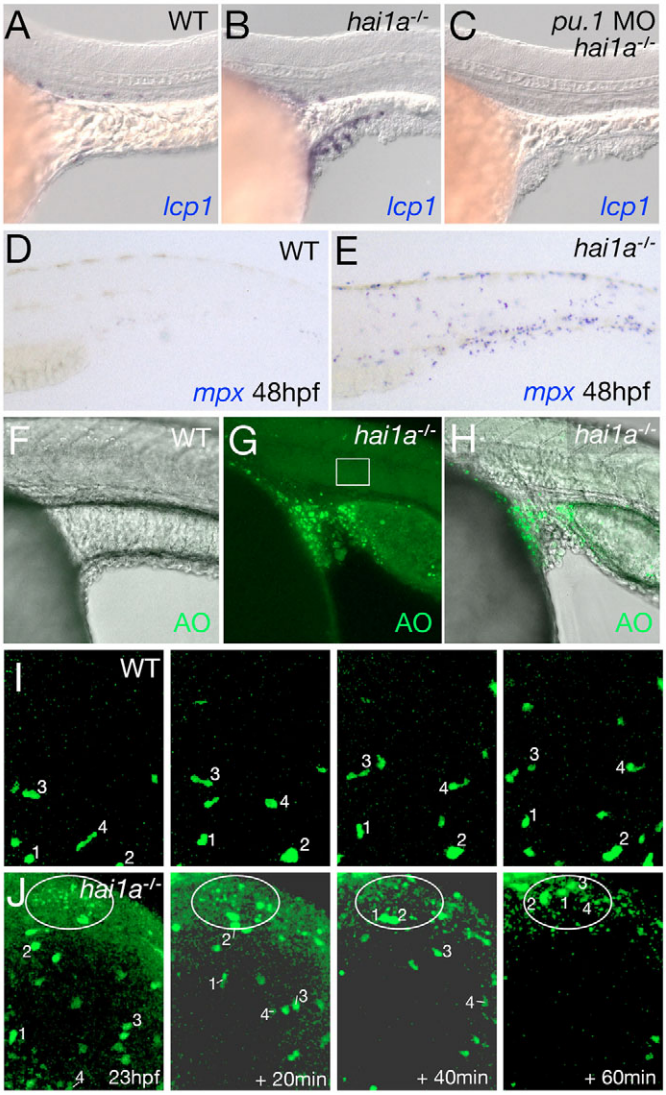

Fig. 6. Skin inflammation in *hai1a* mutants is linked to keratinocyte death, but is dispensable for defects in epithelial integrity. (**A-C**) Lateral views of yolk sac extension of 24 hpf embryos, after in situ hybridization for the leukocyte marker *lcp1*. Leukocytes accumulate around epidermal aggregates in *hai1a* mutants (B); this does not occur in wild-type siblings (WT; A). *hai1a* mutants injected with *pu.1* MO lack leukocytes but display epidermal aggregates of equal severity (C). (**D**,**E**) Lateral trunk views of a wild-type sibling embryo (D) and a *hai1a* mutant (E) after in situ hybridization for the neutrophil marker *mpx* at 48 hpf. (**F-H**) Lateral views of yolk sac extension of a 24 hpf sibling embryo (F) and *hai1a* mutant (G,H), stained with acridine orange (AO). (F,H) Overlays of fluorescent and Nomarski images; (G) fluorescent image. Box in G marks the site where Movie 2 in the supplementary material was taken, stills of which are shown in Fig. 5B. (**I**,**J**) Stills from time-lapse Movies 6 and 7 in the supplementary material (at the indicated times after 23 hpf), demonstrating that *Tg(fli1a:egfp)*-marked leukocytes of *hai1a* mutants migrate from their site of origin anterior to the cardiac field over the yolk sac (Herbomel et al., 1999) to sites with nascent epidermal aggregates and numerous apoptotic cells (J). A cluster of acridine orange (AO)-positive cells is outlined. By comparison, leukocytes of wild-type siblings move more slowly and in a less directed fashion (I). For tracking, four individual leukocytes are indicated with numbers.

morphologically normal, such as the head and the dorsal trunk, displayed normal epithelial characteristics of recorded basal keratinocytes (Fig. 5C; 4/4 movies). By contrast, mesenchymal behavior of basal keratinocytes started significantly earlier (18-20 hpf) in *hai1a, hai1b* double morphants, was more pronounced and was seen throughout the entire epidermis (Fig. 5D; 6/6 movies). We frequently observed keratinocytes crawling on top of each other (Fig. 5E; n=10). We conclude that loss of Hai1 compromises the epithelial integrity of the epidermis and causes keratinocytes to attain an inappropriate mesenchymal-like character and motility, which might account for the observed aggregate formation.

To address epithelial versus mesenchymal properties of epidermal cells with molecular markers, we also carried out immunostainings for the transmembrane adhesion protein E-cadherin. In basal keratinocytes of wild-type embryos at 24 hpf, E-cadherin was localized at the membrane (Fig. 5F). By contrast, in *hai1a* mutant embryos, little to no membranous E-cadherin was detected in basal keratinocytes of the yolk sac or the yolk extension, whereas more E-cadherin signals were obtained in cytoplasmic locations (Fig. 5G). Whole-mount in situ hybridizations and western blotting experiments showed that total *E-cadherin* mRNA and protein levels were unaltered even in *hai1a* mutants injected with *hai1b* MO. By contrast, E-cadherin protein levels were strongly reduced in *smad5*^{dtc24} mutants (Hild et al., 1999), which lack basal keratinocytes, demonstrating that they are the major source of E-cadherin at this stage (Fig. 5H; and data not shown). This suggests that E-cadherin in basal keratinocytes of *hai1* mutants has been redistributed, indicating the loss of epithelial and the incomplete acquisition of mesenchymal properties.

The epidermis of *hai1a* mutants displays enhanced apoptosis and inflammation

In mammals, diseases of the epidermis are often either due to, or invoke, an excessive inflammatory response (Thivolet et al., 1990). To determine whether *hai1a* mutants display similar defects, we examined leukocytes using the in situ markers *leukocyte-specific-plastin* (*lcp1*) (Herbomel et al., 1999; Meijer et al., 2007) and *myeloid-specific peroxidase* (*mpx*) (Lieschke et al., 2001). At 24 hpf, wild-type embryos showed a few leukocytes below the epidermis of the yolk sac and the anterior trunk (Fig. 6A; and data not shown), in concordance with previous reports (Herbomel et al., 2001). *hai1a* mutant embryos at this stage, by contrast, had a strong accumulation of leukocytes over the yolk sac and yolk extension, corresponding to sites of epidermal aggregate formation (Fig. 6B; and data not shown). At later stages (48 hpf), enhanced inflammation was also seen at other sites in *hai1a* mutant embryos, such as the posterior trunk and fins (compare Fig. 6E with 6D).

In order to determine whether this inflammation is causative of the epithelial defects described above, we genetically ablated innate immune cells in *hai1a* mutants by injecting MOs against *pu.1*, which is required for the specification of the myeloid lineage (Rhodes et al., 2005). In situ hybridizations revealed a complete loss of leukocytes in *pu.1* morphant embryos (Fig. 6C). However, epidermal defects of *hai1a* mutants were not ameliorated (Fig. 6C), suggesting that inflammation does not cause, but might instead be induced in parallel to or by, the epidermal defects of *hai1a* mutants.

In several instances, inflammation is induced by dying cells to ensure the proper clearance of apoptotic cell debris by innate immune cells (reviewed in Henson and Hume, 2006). The same

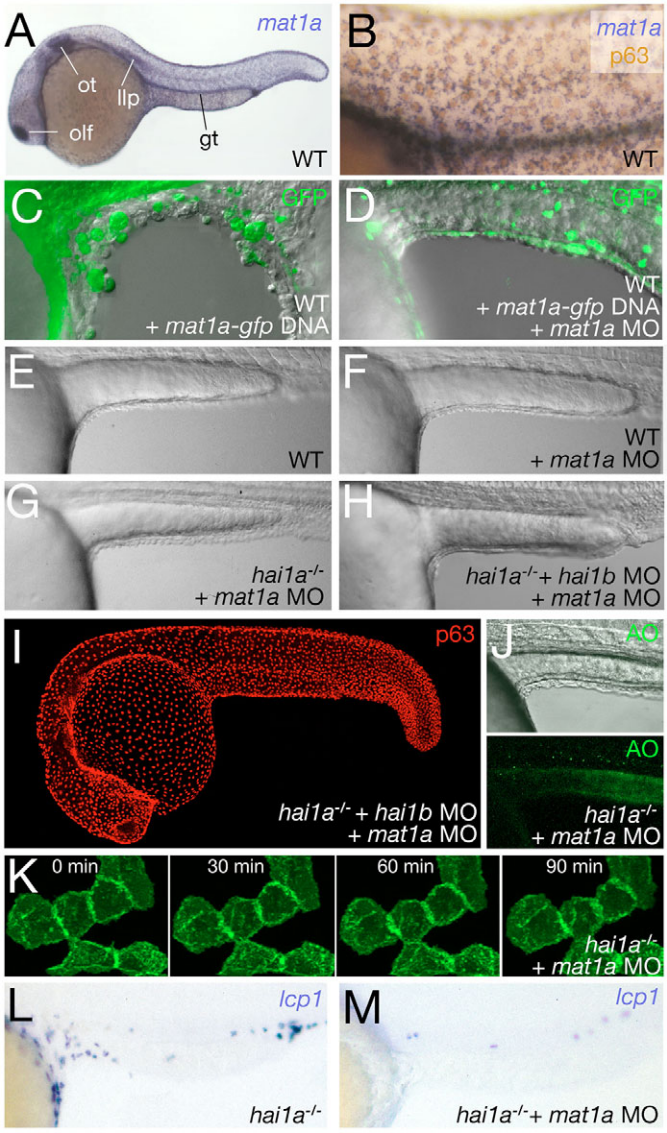

Fig. 7. The defects of *hai1* mutants are phenocopied by overexpression and rescued by knockdown of *matriptase1a*. (**A**) In situ hybridization revealing *matriptase1a* (labelled *mat1a*) expression in the epidermis, olfactory epithelium (olf), otic epithelium (ot), gut (gt) and lateral line primordium (llp) at 24 hpf. (**B**) Counter-staining with p63 antibody (brown), demonstrating expression in the basal epidermal layer. (**C**,**D**) Lateral views of yolk sac extension of heat-shock-treated embryos injected with *pTol2-hse-GTP/matriptase1a* alone (C), displaying epidermal dissociation, or co-injected with *pTol2-hse-GTP/matriptase1a* and *matriptase1a* MO (D), displaying normal epidermal morphology; 24 hpf, overlays of fluorescent and Nomarski images. Cells with transgene expression are labeled by GFP. (**E**,**F**) Lateral Nomarski images of a 24 hpf un-injected wild-type embryo (E) and *matriptase1a* morphant (F), demonstrating that the loss of Matriptase1a does not affect epidermal morphology. (**G**,**H**) Lateral Nomarski images of *hai1a* mutants injected with either *matriptase1a* MO alone (G) or with *matriptase1a* and *hai1b* MOs (H); both display normal epidermal morphology. (**I**) Anti-p63 immunostaining of a 24 hpf *hai1a* mutant co-injected with *matriptase1a* and *hai1b* MOs. (**J**) Acridine orange (AO) staining alone (lower panel) and super-imposed with a Nomarski image (upper panel) of the yolk extension region of a 24 hpf *hai1a* mutant injected with *matriptase1a* MO. (**K**) Stills of time-lapse Movie 8 in the supplementary material (at the times indicated after 24 hpf), demonstrating that *matriptase1a* MO injection restores the epithelial properties of fluorescently labeled *hai1a* morphant basal keratinocytes. (**L**,**M**) Lateral views of the trunk and tail of an un-injected *hai1a* mutant (L) and of a *hai1a* mutant injected with *matriptase1a* MO (M) after in situ hybridization for the leukocyte marker *lcp1* at 24 hpf.

might be true for the epidermal inflammation of *hai1a* mutants. As early as 24 hpf, epidermal aggregates of *hai1a* mutants contained a high number of acridine orange-positive apoptotic keratinocytes (Fig. 6G,H), whereas keratinocyte death was not evident in the epidermis of wild-type embryos (Fig. 6F). Similar results were obtained by TUNEL labeling (data not shown). Time-lapse movies of *hai1a* mutants carrying a *fli1:EGFP* transgene (Redd et al., 2006) further showed that yolk sac leukocytes were strongly attracted by epidermal aggregates with acridine orange-positive cells (Fig. 6J), whereas, in wild-type controls, leukocytes moved more slowly and were less directed (Fig. 6I). In summary, this suggests that epidermal inflammation of *hai1a* mutants is secondarily caused by the death of keratinocytes.

hai1 mutant epidermal defects are phenocopied by overexpression and rescued by inactivation of Matriptase1a

Hai1 is known to inhibit a number of serine proteases, including the membrane bound protease Matriptase1. To ascertain whether this target was implicated in the *hai1* mutant phenotype, we identified and cloned two zebrafish *matriptase1* orthologs – *matriptase1a* (*st14a*; GenBank accession number BC115342) and *matriptase1b* (*st14b*; GenBank accession number BC125837). While *matriptase1b* was expressed in the central nervous system (data not shown), *matriptase1a* showed strong epidermal expression starting at approximately 18 hpf, immediately prior to the onset of the *hai1* mutant phenotype. Expression at 24 hpf appeared notably similar to that of *hai1a,* with transcripts in the basal layer of the epidermis, the otic vesicle, the olfactory epithelium and the gut (Fig. 7A,B).

To test whether the epidermal defects of *hai1* mutants might be due to a lack of Matriptase1a inhibition, we attempted to phenocopy and rescue the defects by Matripase1a overexpression or inactivation, respectively. Heat-treated wild-type embryos that had been injected with *pTol2-hse-GTP/matriptase1a* DNA (see Materials and methods) displayed severe dissociation of GFP-positive keratinocytes and skin aggregate formation both in dorsal (data not shown) and ventral (Fig. 7C; *n*=7/8 embryos with GFP-positive keratinocytes) positions, similar to the phenotype of *hai1* mutants/morphants (Fig. 3). Defects were rescued to wild-type condition upon co-injection of *pTol2-hse-GTP/matriptase1a* with an MO targeting the *matriptase1a* translation start site (Fig. 7D; *n*=0/6 embryos with GFP-positive keratinocytes), indicating that they are indeed due to a gain of Matriptase1a activity. Similarly, whereas the knockdown of Matriptase1a in wild-type embryos had no effect (compare Fig. 7F with Fig. 7E), *hai1a, matriptase1a* double- and *hai1a, hai1b, matriptase1a* triple-mutant/morphant embryos displayed a robust rescue of the *hai1* mutant phenotype, with epidermal morphology indistinguishable from that of wild-type siblings (compare Fig. 7G,H with Fig. 3E,N; Table 1). In particular, basal keratinocytes did not form aggregates and were not shed, but maintained their even distribution, as was seen in wild-type embryos (compare Fig. 7I with Fig. 3F,O). Similarly, in vivo imaging revealed

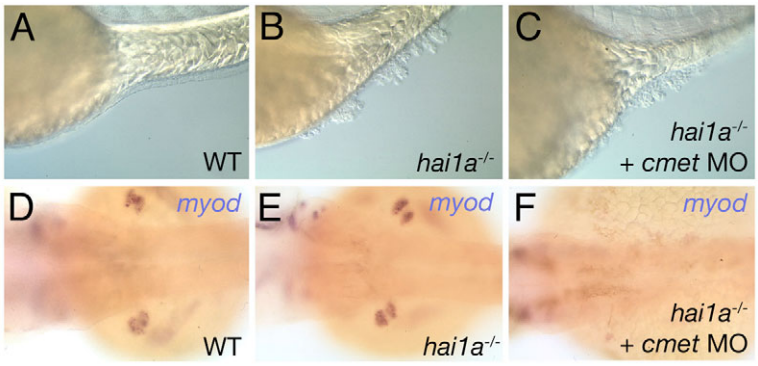

Fig. 8. Inactivation of Met fails to rescue epithelial defects in *hai1a* mutants. (**A-C**) Lateral Nomarski images of a wild-type sibling (WT; A), *hai1a* mutant (B) and *met* (*cmet*) MO-injected *hai1a* mutant (C) at 48 hpf, revealing the presence of epidermal aggregates both in injected (C) and un-injected (B) mutants. (**D-F**) Dorsal views of the trunk region of embryos shown in A-C, with the pectoral fin muscle labeled for *myoD* transcripts. The pectoral fin muscle is absent from the *met* morphant (F), compared with un-injected siblings (D,E), demonstrating that the MO is functional. Notice the presence of normal pectoral fin muscle in the *hai1a* mutant (E), indicating that Hai1a is dispensable for the Hgf- and Met-dependent migration of fin muscle precursor cells (Haines et al., 2004).

that keratinocytes dorsal of the yolk extension of *matriptase1a*-MO-injected *hai1a* mutants maintained epithelial properties (Fig. 7K; 4/4 movies of transplanted cells), in contrast to the acquisition of mesenchymal-like characteristics in *hai1a* mutants at this location, as described above (Fig. 5B). Furthermore, apoptosis of keratinocytes was suppressed (compare Fig. 7J with Fig. 6G,H), as was skin inflammation (compare Fig. 7M with 7L). In conclusion, all phenotypic traits caused by the loss of Hai1 activity could be rescued by concomitant inactivation of Matriptase1a, indicating that, during normal development, Hai1 promotes skin homeostasis by blocking Matriptase1a activity.

Enhanced signaling via Hgf-Met does not account for the *hai1a* mutant phenotype

Biochemical studies have identified multiple extracellular target proteins of Matriptase1. A prominent example is Hgf, which, upon binding to its receptor, Met, can induce epithelial scattering and epithelial-mesenchymal transitions (EMT). In vitro, Matriptase1 can proteolytically cleave the biologically inactive Hgf precursor protein, thereby releasing mature Hgf. Inactivation of the zebrafish Met or Hgf orthologs via MO or antibody injection abrogates the migration of pectoral fin muscle precursors and presumptive neuromasts of the lateral line system (Haines et al., 2004). To study whether elevated Hgf signaling might account for the loss of epithelial integrity seen in the *hai1a* mutant epidermis, we injected *hai1a* mutants with *met* MO. However, in contrast to Matriptase1a (Fig. 7G), knockdown of Met activity did not alleviate epidermal aggregate formation (compare Fig. 8C with 8A,B) or inflammation (data not shown), although embryos lacked pectoral fin muscles (compare Fig. 8F with 8D,E), demonstrating that the MO was functional. To discount potential redundancies with other related receptors, we also cloned zebrafish orthologs of the closely related mammalian Ron receptor (GenBank accession number CF997695) and a Ron-relative most similar to avian Sea and Fugu rubripes, Prgfr3 [Plasminogen related growth factor receptor 3 (Cottage et al., 1999); GenBank accession number EF424429]. However, we were unable to detect expression of any of these receptor genes in the zebrafish epidermis at 24 hpf (data not shown). Furthermore, co-injection of MOs against all three members of this receptor family (Met, Ron and Prgfr3) failed to rescue the skin defects of *hai1a* mutants (see Fig. S2E-H in the supplementary material), although all MOs efficiently suppressed the translation of their respective mRNA upon co-injection (see Fig. S2A-D in the supplementary material). We conclude that the defects caused by the loss of Hai1 and gain of Matriptase1a activity are not due to enhanced signaling via the Hgf receptor Met or any of its relatives.

DISCUSSION

Zebrafish *hai1* is essential for skin development and embryonic survival

In the mouse, Hai1-mediated inhibition of Matriptase1 is required for proper placenta formation, with mutant embryos resorbing at embryonic day (E)12 (Tanaka et al., 2005). These early defects have precluded studies on possible other essential roles of Hai1 during later development, such as in the skin. The recent observation that *Hai1, Matriptase1* double-mutant mice develop to term (Szabo et al., 2007) and only show skin defects associated with the loss of Matriptase1 (List et al., 2002; List et al., 2003) could have two meanings. It could indicate either that Hai1 is dispensable for other developmental processes, or that, as in the placenta, the role of Hai1 in such other tissues is to block Matriptase1. Tissue-specific knock-out of the mouse *Hai1* gene would be necessary to distinguish between these two possibilities.

Here, we have analyzed the skin phenotype caused by loss of Hai1 function in a non-placental vertebrate, the zebrafish. Skin defects of *hai1a* mutants are most prominent around 24-26 hpf, but recover to almost wild-type condition during further development. By contrast, combined loss of Hai1a and its paralog, Hai1b, which, per se, is dispensable, causes a much stronger phenotype, characterized by a dissociation of the entire epidermis and embryonic death between 18 and 26 hpf. Both the moderate defects of *hai1a* mutants and the stronger defects of *hai1a* mutants or morphants injected with *hai1b* MO were rescued upon injection of a *matriptase1a*-specific MO, indicating that Hai1a and Hai1b act in partial redundancy and by blocking Matriptase1a activity. Our data are in line with results obtained upon transgene-driven overexpression of Matriptase1 in mouse keratinocytes, which leads to epidermal hyperplasia, skin inflammation and heightened tumorigenicity in the adult epidermis, all of which can be suppressed upon concomitant skin-specific overexpression of *Hai1* (List et al., 2005). In addition to providing the first direct proof for an indispensable role of Hai1 in the vertebrate epidermis, our data also highlight that the primary function of Hai1 is concerned with the maintenance of epithelial integrity within the basal epidermal layer, whereas skin inflammation and epidermal hyperplasia appear to be secondary consequences.

Keratinocyte aggregate formation and shedding in *hai1* mutants result from a loss of epithelial integrity

At 24 hpf, aggregation and shedding of keratinocytes in *hai1a*$^{-/-}$ homozygotes was largely restricted to the ventral side of the embryo, and most prominent on the yolk sac and the forming yolk extension, whereas, at 36 hpf, aggregates were mainly found on the outgrowing

body fins. These are the regions of the embryo with the most-pronounced morphological changes, suggesting that here, the epidermis is exposed to highest mechanical stress and undergoes tissue remodeling even during normal development. Such remodeling processes most probably involve a transient loss of epithelial properties of keratinocytes, which might be driven by Matriptase1a. If so, however, it remains unclear why the loss of Matriptase1a activity does not cause developmental defects. Functional redundancy with other serine proteases could be one explanation. In addition, Matriptase1a might only become essential for tissue remodeling that occurs during pathological conditions, such as wound healing. To test this notion, we compared wound healing in wild-type and *matriptase1a* morphant larvae, which, at this stage, normally involves actin cable-driven purse-string contractions of keratinocytes, as in mammalian embryos (Redd et al., 2004). This process occurred normally in wounded *matriptase1a* morphants, (T.J.C. and M.H., unpublished observations). Further analyses are necessary, including wound-healing studies of *matriptase1a* mutants during adulthood, when cutaneous wound closure involves EMT of keratinocytes (T.J.C., Krasimir Slanchev and M.H., unpublished observations).

Nonetheless, our in vivo time-lapse recordings of fluorescently labeled *hai1a* mutant keratinocytes revealed that, during development, these cells have the potential to become mesenchymal. We observed such behavior, localized to ventral regions, in *hai1a* single mutants at 24 hpf, whereas the loss of both Hai1a and Hai1b led to the enhanced, earlier and more-widespread acquisition of mesenchymal-like properties of basal keratinocytes. In these movies, we also observed mutant basal keratinocytes crawling on top of each other. Furthermore, mesenchymal-like behavior was observed in keratinocytes far removed from aggregates, suggesting that the acquisition of fibroblastoid properties and motility is causative, rather than a secondary consequence, of aggregate formation.

It is important to note that *hai1* mutant keratinocytes did not become completely mesenchymal. Thus, they lacked the mesenchymal marker Vimentin (T.J.C. and M.H., unpublished data). In addition, mRNA and protein levels of the epithelial marker E-cadherin remained unchanged. However, E-cadherin protein appeared to be redistributed, indicating a loss of epithelial polarity. Acquisition of fibroblastoid shapes and motility under such conditions is sometimes termed 'scattering', in reference to its initial discovery as an effect induced by Scatter factor (Sf, identical to Hgf), and is opposed to complete EMTs, which require additional and/or prolonged signaling (for a review, see Grünert et al., 2003).

Keratinocyte apoptosis, skin inflammation and epidermal hyperplasia of *hai1* mutants are secondary consequences of the loss of epithelial integrity

In addition to keratinocyte scattering, loss of Hai1 activity leads to keratinocyte death, enhanced skin inflammation and epidermal hyperplasia. Although the phenotype caused by the combined loss of Hai1a and Hai1b was too severe to dissect these traits, analyses of *hai1a* single mutants suggest that all are secondary consequences of the loss of epithelial integrity. Thus, apoptosis of keratinocytes was usually observed only in the most severely affected regions and within cell aggregates, whereas keratinocyte scattering was also recorded in regions devoid of dying cells. This suggests that keratinocyte death might be a secondary consequence of their detachment from the basement membrane when they pile up on each other, a phenomenon called anoikis, which has been well characterized in vitro (Gilmore, 2005). This death of keratinocytes might in turn induce skin inflammation, characterized by enhanced numbers of leukocytes in the *hai1a* mutant skin. Strikingly, the spatial pattern of inflammation resembled that of keratinocyte apoptosis (compare Fig. 6B with 6G). Whereas apoptosis preceded inflammation and had its peak between 24 and 28 hpf, inflammation continued beyond 48 hpf. Furthermore, time-lapse recordings revealed that innate immune cells were strongly attracted by apoptotic keratinocytes. Ultimate proof for a causative relationship between keratinocyte death and inflammation would require analysis of inflammation in *hai1a* mutants after the suppression of cell death. For this purpose, we injected mutants with MOs targeting the pro-apoptotic transcription factor p53 (Plaster et al., 2006) or with mRNA encoding the anti-apoptotic Bcl-2 protein (Langenau et al., 2005). However, both treatments failed to lower the number of dying keratinocytes in *hai1a* mutants (T.J.C. and M.H., unpublished data), suggesting that keratinocyte death is accomplished independently of the intrinsic, and possibly driven by the extrinsic, apoptosis pathway [compare with Rytomaa et al. (Rytomaa et al., 1999)]. Although it cannot be ruled out that inflammation in *hai1a* is induced by other means in parallel to dying keratinocytes, we can rule out that inflammation is causative of the epithelial defects, because they persisted in *hai1a* mutants after genetic ablation of all innate immune cells by *pu.1*-MO injection.

Finally, our BrdU-incorporation studies indicate that proliferation of keratinocytes is only secondarily affected, most probably due to the loss of epithelial integrity and possibly contact inhibition. Thus, at 24 hpf, keratinocyte aggregates in *hai1* mutants were solely composed of non-proliferating cells, whereas keratinocyte hyper-proliferation was only seen later and after the onset all other phenotypic traits (48 hpf). Similarly, transgenic mice overexpressing Matriptase1 in keratinocytes display late epidermal hyperplasia in vivo, although isolated keratinocytes show normal proliferative behavior when cultured in vitro (List et al., 2005), arguing for an indirect effect of the Hai1-Matriptase1 system on cell proliferation.

What are the substrates of Matriptase1 accounting for the epidermal defects in *hai1* mutants?

Biochemical analyses have identified multiple Matriptase1 substrate proteins; among them is Hgf, which is involved in the regulation of several epithelial-mesenchymal transitions during vertebrate development (for a review, see Birchmeier and Gherardi, 1998) and which requires Matriptase1- or Hgfa-mediated proteolytic cleavage to become biologically active. This suggests that the epithelial defects of *hai1* mutants might be due to Matriptase1-mediated upregulation of Hgf activity. Furthermore, applied Hgf has been shown to attract innate immune cells to skin wounds (Bevan et al., 2004), suggesting that elevated Hgf activity might also account for the observed skin inflammation of *hai1* mutants. Additionally, Hai1 and Matriptase1 could act via other related ligands such as Mst1 (Macrophage-stimulating protein), shown to stimulate chemotactic migration of macrophages (Leonard and Skeel, 1978) as well as keratinocyte mobility (Santoro et al., 2003). Indeed, a zebrafish *mst1* homolog has been reported to be highly expressed on the yolk sac and the yolk extension (Bassett, 2003), the two most strongly affected sites of *hai1a* mutants. However, knockdown of the Hgf receptor Met (Haines et al., 2004), the Mst1 receptor Ron (Gaudino et al., 1994) and the related Plasminogen related growth factor receptor 3 (Cottage et al., 1999) failed to rescue the epidermal defects of *hai1a* mutants. This strongly suggests that Hai1 and Matriptase1a regulate skin homeostasis and remodeling via other or additional proteins.

A recent report on the placental phenotype of *Hai1* mutant mice has described compromised basement membrane integrity (Fan et al., 2007), suggesting that epithelial defects might be due to increased degradation of Laminins, other described Matriptase1 substrate proteins (see Introduction). However, whole-mount immunostainings and western blotting experiments of *hai1a* mutant and *hai1a, hai1b* double-deficient embryos revealed unchanged Laminin protein levels and cleavage patterns (T.J.C. and M.H., unpublished data), suggesting that the epidermal defects are not due to direct alterations in Laminin processing.

In conclusion, although we can exclude some of the most obvious candidates as the prime or sole Matriptase1 target proteins, the crucial players downstream of Matriptase1, accounting for the epidermal defects caused by the loss of Hai1 activity, remain elusive. Systematic antisense-mediated knockdowns of other candidates in *hai1a* zebrafish mutants, as well as genetic *hai1a* suppressor screens, are in preparation to hopefully reveal the nature of these proteins in the future.

We are very grateful to John Kanki and A. Thomas Look (*mpx*, *pu.1* MO); Thomas Czerny (pSGH2); Koichi Kawakami (pT2AL200R150G); and Christine and Bernard Thisse (*lcp1*) for sending reagents. The *Tg(bactin:hras-egfp)* line was generated by J.T. while he was a postdoctoral fellow in the laboratory of Lilianna Solnica-Krezel. Work in the laboratory of M.H. was supported by the Max-Planck Society, by the European Union (6th framework integrated project 'Zebrafish models for human development and disease') and by the National Institutes of Health (NIH grant 1R01-GM63904). Work in N.H.'s laboratory was supported by a grant from the National Center for Research Resources at the National Institutes of Health (2R01-RR012589-6).

Supplementary material

Supplementary material for this article is available at http://dev.biologists.org/cgi/content/full/134/19/3461/DC1

References

Ahmed, S., Jin, X., Yagi, M., Yasuda, C., Sato, Y., Higashi, S., Lin, C. Y., Dickson, R. B. and Miyazaki, K. (2006). Identification of membrane-bound serine proteinase matriptase as processing enzyme of insulin-like growth factor binding protein-related protein-1 (IGFBP-rP1/angiomodulin/mac25). *FEBS J.* **273**, 615-627.

Amsterdam, A., Burgess, S., Golling, G., Chen, W., Sun, Z., Townsend, K., Farrington, S., Haldi, M. and Hopkins, N. (1999). A large-scale insertional mutagenesis screen in zebrafish. *Genes Dev.* **13**, 2713-2724.

Amsterdam, A., Nissen, R. M., Sun, Z., Swindell, E. C., Farrington, S. and Hopkins, N. (2004). Identification of 315 genes essential for early zebrafish development. *Proc. Natl. Acad. Sci. USA* **101**, 12792-12797.

Babb, S. G., Barnett, J., Doedens, A. L., Cobb, N., Liu, Q., Sorkin, B. C., Yelick, P. C., Raymond, P. A. and Marrs, J. A. (2001). Zebrafish E-cadherin: expression during early embryogenesis and regulation during brain development. *Dev. Dyn.* **221**, 231-237.

Bajoghli, B., Aghaallaei, N., Heimbucher, T. and Czerny, T. (2004). An artificial promoter contruct for heat-inducible misexpression during zebrafish embryogenesis. *Dev. Biol.* **271**, 416-430.

Bakkers, J., Hild, M., Kramer, C., Furutani-Seiki, M. and Hammerschmidt, M. (2002). Zebrafish ΔNp63 is a direct target of Bmp signaling and encodes a transcriptional repressor blocking neural specification in the ventral ectoderm. *Dev. Cell* **2**, 617-627.

Bassett, D. I. (2003). Identification and developmental expression of a *macrophage stimulating/hepatocyte growth factor-like 1* orthologue in zebrafish. *Dev. Genes Evol.* **213**, 360-362.

Benaud, C., Dickson, R. B. and Lin, C. Y. (2001). Regulation of the activity of matriptase on epithelial cell surfaces by a blood-derived factor. *Eur. J. Biochem.* **268**, 1439-1447.

Bevan, D., Gherardi, E., Fan, T.-P., Edwards, D. and Warn, R. (2004). Diverse and potent activities of HGF/SF in skin wound repair. *J. Pathol.* **203**, 831-838.

Bhatt, A. S., Erdjument-Bromage, H., Tempst, P., Craik, C. S. and Moasser, M. M. (2005). Adhesion signaling by a novel mitotic substrate of src kinases. *Oncogene* **24**, 5333-5343.

Birchmeier, C. and Gherardi, E. (1998). Developmental roles of HGF/SF and its receptor, the c-Met tyrosine kinase. *Trends Cell Biol.* **8**, 404-410.

Cooper, M. S., Szeto, D. P., Sommers-Herivel, G., Topczewski, J., Solnica-Krezel, L., Kang, H. C., Johnson, I. and Kimelman, D. (2005). Visualizing morphogenesis in transgenic zebrafish embryos using BODIPY TR methyl ester dye as a vital counterstain for GFP. *Dev. Dyn.* **232**, 359-368.

Cottage, A., Clark, M., Hawker, K., Umrania, Y., Wheller, D., Bishop, M. and Elgar, G. (1999). Three receptor genes for plasminogen related growth factors in the genome of the puffer fish Fugu rubripes. *FEBS Lett.* **443**, 370-374.

Denda, K., Shimomura, T., Kawaguchi, T., Miyazawa, K. and Kitamura, N. (2002). Functional characterization of Kunitz domains in hepatocyte growth factor activator inhibitor type 1. *J. Biol. Chem.* **277**, 14053-14059.

Fan, B., Brennan, J., Grant, D., Peale, F., Rangell, L. and Kirchhofer, D. (2007). Hepatocyte growth factor activator inhibitor-1 (HAI-1) is essential for the integrity of basement membranes in the developing placental labyrinth. *Dev. Biol.* **303**, 222-230.

Forbs, D., Thiel, S., Stella, M. C., Sturzebecher, A., Schweinitz, A., Steinmetzer, T., Sturzebecher, J. and Uhland, K. (2005). In vitro inhibition of matriptase prevents invasive growth of cell lines of prostate and colon carcinoma. *Int. J. Oncol.* **27**, 1061-1070.

Furutani-Seiki, M., Jiang, Y. J., Brand, M., Heisenberg, C. P., Houart, C., Beuchle, D., van Eeden, F. J., Granato, M., Haffter, P., Hammerschmidt, M. et al. (1996). Neural degeneration mutants in the zebrafish, Danio rerio. *Development* **123**, 229-239.

Gaudino, G., Follenzi, A., Naldini, L., Collesi, C., Santoro, M., Gallo, K. A., Godowski, P. J. and Comoglio, P. M. (1994). RON is a heterodimeric tyrosine kinase receptor activated by the HGF homologue MSP. *EMBO J.* **13**, 3524-3532.

Gilmore, A. P. (2005). Anoikis. *Cell Death Differ.* **12** Suppl. 2, 1473-1477.

Grünert, G., Jechlinger, M. and Beug, H. (2003). Diverse cellular and molecular mechanisms contribute to epithelial plasticity and metastasis. *Nat. Rev. Mol. Cell Biol.* **4**, 657-665.

Haines, L., Neyt, C., Gautier, P., Keenan, D. G., Bryson-Richardson, R. J., Hollway, G. E., Cole, N. J. and Currie, P. D. (2004). Met and Hgf signaling controls hypaxial muscle and lateral line development in the zebrafish. *Development* **131**, 4857-4869.

Hammerschmidt, M., Pelegri, F., Mullins, M. C., Kane, D. A., van Eeden, F. J., Granato, M., Brand, M., Furutani-Seiki, M., Haffter, P., Heisenberg, C. P. et al. (1996). dino and mercedes, two genes regulating dorsal development in the zebrafish embryo. *Development* **123**, 95-102.

Henson, P. M. and Hume, D. A. (2006). Apoptotic cell removal in development and tissue homeostasis. *Trends Immunol.* **27**, 244-250.

Herbomel, P., Thisse, B. and Thisse, C. (1999). Ontogeny and behaviour of early macrophages in the zebrafish embryo. *Development* **126**, 3735-3745.

Herbomel, P., Thisse, B. and Thisse, C. (2001). Zebrafish early macrophages colonize cephalic mesenchyme and developing brain, retina, and epidermis through a M-CSF receptor-dependent invasive process. *Dev. Biol.* **238**, 274-288.

Hild, M., Dick, A., Rauch, G.-J., Meier, A., Bouwmeester, T., Haffter, P. and Hammerschmidt, M. (1999). The smad5 mutation somitabun blocks Bmp2b signaling during early dorsoventral patterning of the zebrafish embryo. *Development* **126**, 2149-2159.

Jin, X., Yagi, M., Akiyama, N., Hirosaki, T., Higashi, S., Lin, C. Y., Dickson, R. B., Kitamura, H. and Miyazaki, K. (2006). Matriptase activates stromelysin (MMP-3) and promotes tumor growth and angiogenesis. *Cancer Sci.* **97**, 1327-1334.

Kataoka, H., Itoh, H. and Koono, M. (2002). Emerging multifunctional aspects of cellular serine proteinase inhibitors in tumor progression and tissue regeneration. *Pathol. Int.* **52**, 89-102.

Kawakami, K., Takeda, H., Kawakami, N., Kobayashi, M., Matsuda, N. and Mishina, M. (2004). A transposon-mediated gene trap approach identifies developmentally regulated genes in zebrafish. *Dev. Cell* **7**, 133-144.

Kim, M. G., Chen, C., Lyu, M. S., Cho, E. G., Park, D., Kozak, C. and Schwartz, R. H. (1999). Cloning and chromosomal mapping of a gene isolated from thymic stromal cells encoding a new mouse type II membrane serine protease, epithin, containing four LDL receptor modules and two CUB domains. *Immunogenetics* **49**, 420-428.

Kirchhofer, D., Peek, M., Li, W., Stamos, J., Eigenbrot, C., Kadkhodayan, S., Elliott, J. M., Corpuz, R. T., Lazarus, R. A. and Moran, P. (2003). Tissue expression, protease specificity, and Kunitz domain functions of hepatocyte growth factor activator inhibitor-1B (HAI-1B), a new splice variant of HAI-1. *J. Biol. Chem.* **278**, 36341-36349.

Langenau, D. M., Jette, C., Berghmans, S., Palomero, T., Kanki, J. P., Kutok, J. L. and Look, A. T. (2005). Suppression of apoptosis by bcl-2 overexpression in lymphoid cells of transgenic zebrafish. *Blood* **105**, 3278-3285.

Lawson, N. D. and Weinstein, B. M. (2002). In vivo imaging of embryonic vascular development using transgenic zebrafish. *Dev. Biol.* **248**, 307-318.

Le Guellec, D., Morvan-Dubois, G. and Sire, J.-Y. (2004). Skin development in bony fish with particular emphasis on collagen deposition in the dermis of zebrafish (*Danio rerio*). *Int. J. Dev. Biol.* **48**, 217-231.

Lee, H. and Kimelman, D. (2002). A dominant-negative form of p63 is required for epidermal proliferation in zebrafish. *Dev. Cell* **2**, 607-616.

Lee, S. L., Dickson, R. B. and Lin, C. Y. (2000). Activation of hepatocyte growth factor and urokinase/plasminogen activator by matriptase, an epithelial membrane serine protease. *J. Biol. Chem.* **275**, 36720-36725.

Leonard, E. J. and Skeel, A. H. (1978). Isolation of macrophage stimulating protein (MSP) from human serum. *Exp. Cell Res.* **114**, 117-126.

Lieschke, G. J., Oates, A. C., Crowhurst, M. O., Ward, A. C. and Layton, J. E.

(2001). Morphologic and functional characterization of granulocytes and macrophages in embryonic and adult zebrafish. *Blood* **98**, 3087-3096.
Lieschke, G. J., Oates, A. C., Paw, B. H., Thompson, M. A., Hall, N. E., Ward, A. C., Ho, R. K., Zon, L. I. and Layton, J. E. (2002). Zebrafish SPI-1 (PU.1) marks a site of myeloid development independent of primitive erythropoiesis: implications for axial patterning. *Dev. Biol.* **246**, 274-295.
Lin, C. Y., Anders, J., Johnson, M. and Dickson, R. B. (1999a). Purification and characterization of a complex containing matriptase and a Kunitz-type serine protease inhibitor from human milk. *J. Biol. Chem.* **274**, 18237-18242.
Lin, C. Y., Anders, J., Johnson, M., Sang, Q. A. and Dickson, R. B. (1999b). Molecular cloning of cDNA for matriptase, a matrix-degrading serine protease with trypsin-like activity. *J. Biol. Chem.* **274**, 18231-18236.
List, K., Haudenschild, C. C., Szabo, R., Chen, W., Wahl, S. M., Swaim, W., Engelholm, L. H., Behrendt, N. and Bugge, T. H. (2002). Matriptase/MT-SP1 is required for postnatal survival, epidermal barrier function, hair follicle development, and thymic homeostasis. *Oncogene* **21**, 3765-3779.
List, K., Szabo, R., Wertz, P. W., Segre, J., Haudenschild, C. C., Kim, S. Y. and Bugge, T. H. (2003). Loss of proteolytically processed filaggrin caused by epidermal deletion of Matriptase/MT-SP1. *J. Cell Biol.* **163**, 901-910.
List, K., Szabo, R., Molinolo, A., Sriuranpong, V., Redeye, V., Murdock, T., Burke, B., Nielsen, B. S., Gutkind, J. S. and Bugge, T. H. (2005). Deregulated matriptase causes ras-independent multistage carcinogenesis and promotes ras-mediated malignant transformation. *Genes Dev.* **19**, 1934-1950.
List, K., Bugge, T. H. and Szabo, R. (2006). Matriptase: potent proteolysis on the cell surface. *Mol. Med*. **12**, 1-7.
Meijer, A. H., van der Sar, A. M., Cunha, C., Lamers, G. E. M., Laplante, M. A., Kikuta, H., Bitter, W., Becker, T. S. and Spaink, H. P. (2007). Identification and real-time imaging of a *myc*-expressing neutrophil population involved in inflammation and mycobacterial granuloma formation in zebrafish. *Dev. Comp. Immunol*. doi:10.1016/j.dci.2007.04.003.
Nasevicius, A. and Ekker, S. C. (2000). Effective targeted gene 'knockdown' in zebrafish. *Nat. Genet.* **26**, 216-220.
Oberst, M., Anders, J., Xie, B., Singh, B., Ossandon, M., Johnson, M., Dickson, R. B. and Lin, C. Y. (2001). Matriptase and HAI-1 are expressed by normal and malignant epithelial cells in vitro and in vivo. *Am. J. Pathol.* **158**, 1301-1311.
Oberst, M. D., Singh, B., Ozdemirli, M., Dickson, R. B., Johnson, M. D. and Lin, C. Y. (2003). Characterization of matriptase expression in normal human tissues. *J. Histochem. Cytochem.* **51**, 1017-1025.
Parr, C. and Jiang, W. G. (2006). Hepatocyte growth factor activation inhibitors (HAI-1 and HAI-2) regulate HGF-induced invasion of human breast cancer cells. *Int. J. Cancer* **119**, 1176-1183.
Plaster, N., Sonntag, C., Busse, C. E. and Hammerschmidt, M. (2006). p53 deficiency rescues apoptosis and differentiation of multiple cell types in zebrafish flathead mutants deficient for zygotic DNA polymerase delta1. *Cell Death Differ.* **13**, 223-235.
Postlethwait, J. H., Yan, Y.-L., Gates, M. A., Horne, S., Amores, A., Brownlie, A., Donovan, A., Egan, E. S., Force, A., Gong, Z. et al. (1998). Vertebrate genome evolution and the zebrafish gene map. *Nat. Genet.* **18**, 345-349.
Redd, M. J., Cooper, L., Wood, W., Stramer, B. and Martin, P. (2004). Wound healing and inflammation: embryos reveal the way of perfect repair. *Philos. Trans. R. Soc. Lond. B Biol. Sci.* **359**, 777-784.
Redd, M. J., Kelly, G., Dunn, G., Way, M. and Martin, P. (2006). Imaging macrophage chemotaxis in vivo: studies of microtubule function in zebrafish wound inflammation. *Cell Motil. Cytoskeleton* **63**, 415-422.
Rhodes, J., Hagen, A., Hsu, K., Deng, M., Liu, T. X., Look, A. T. and Kanki, J. P. (2005). Interplay of pu.1 and gata1 determines myelo-erythroid progenitor cell fate in zebrafish. *Dev. Cell* **8**, 97-108.
Rytomaa, M., Martins, L. M. and Downward, J. (1999). Involvement of FADD and caspase-8 signalling in detachment-induced apoptosis. *Curr. Biol.* **9**, 1043-1046.
Santoro, M. M., Gaudino, G. and Marchisio, P. C. (2003). The MSP receptor regulates alpha6beta4 and alpha3beta1 integrins via 14-3-3 proteins in keratinocyte migration. *Dev. Cell* **5**, 257-271.
Satomi, S., Yamasaki, Y., Tsuzuki, S., Hitomi, Y., Iwanaga, T. and Fushiki, T. (2001). A role for membrane-type serine protease (MT-SP1) in intestinal epithelial turnover. *Biochem. Biophys. Res. Commun.* **287**, 995-1002.
Shi, Y. E., Torri, J., Yieh, L., Wellstein, A., Lippman, M. E. and Dickson, R. B. (1993). Identification and characterization of a novel matrix-degrading protease from hormone-dependent human breast cancer cells. *Cancer Res.* **53**, 1409-1415.
Shimomura, T., Denda, K., Kitamura, A., Kawaguchi, T., Kito, M., Kondo, J., Kagaya, S., Qin, L., Takata, H., Miyazawa, K. et al. (1997). Hepatocyte growth factor activator inhibitor, a novel Kunitz-type serine protease inhibitor. *J. Biol. Chem.* **272**, 6370-6376.
Sonawane, M., Carpio, Y., Geisler, R., Schwarz, H., Maischein, H. M. and Nüsslein-Volhard, C. (2005). Zebrafish *penner/lethal giant larvae 2* functions in hemidesomosome formation, maintenance of cellular morphology and growth regulation in the developing basal epidermis. *Development* **132**, 3255-3265.
Szabo, R., Molinolo, A., List, K. and Bugge, T. H. (2007). Matriptase inhibition by hepatocyte growth factor activator inhibitor-1 is essential for placental development. *Oncogene* **26**, 1546-1556.
Takeuchi, T., Shuman, M. A. and Craik, C. S. (1999). Reverse biochemistry: use of macromolecular protease inhibitors to dissect complex biological processes and identify a membrane-type serine protease in epithelial cancer and normal tissue. *Proc. Natl. Acad. Sci. USA* **96**, 11054-11061.
Takeuchi, T., Harris, J. L., Huang, W., Yan, K. W., Coughlin, S. R. and Craik, C. S. (2000). Cellular localization of membrane-type serine protease 1 and identification of protease-activated receptor-2 and single-chain urokinase-type plasminogen activator as substrates. *J. Biol. Chem.* **275**, 26333-26342.
Tanaka, H., Nagaike, K., Takeda, N., Itoh, H., Kohama, K., Fukushima, T., Miyata, S., Uchiyama, S., Uchinokura, S., Shimomura, T. et al. (2005). Hepatocyte growth factor activator inhibitor type 1 (HAI-1) is required for branching morphogenesis in the chorioallantoic placenta. *Mol. Cell. Biol.* **25**, 5687-5698.
Thivolet, J., Nicolas, J. F. and Faure, M. (1990). Patholphysiology: immunological mechanisms in dermatological diseases. In *Skin Immune System (SIS)* (ed. J. D. Bos), pp. 355-379. Boca Raton, FL: CRC Press.
Urasaki, A., Morvan, G. and Kawakami, K. (2006). Functional dissection of the Tol2 transposable element identified the minimal cis-sequence and a highly repetitive sequence in the subterminal region essential for transposition. *Genetics* **174**, 639-649.
Weinberg, E. S., Allende, M. L., Kelly, C. S., Abdelhamid, A., Murakami, T., Andermann, P., Doerre, O. G., Grunwald, D. J. and Riggleman, B. (1996). Developmental regulation of zebrafish *myoD* in wild-type, *no tail* and *spadetail* embryos. *Development* **122**, 271-280.